

© 2020. U. Marmol, N. Borowiec.

This is an open-access article distributed under the terms of the Creative Commons Attribution-NonCommercial-NoDerivatives License (CC BY-NC-ND 4.0, <https://creativecommons.org/licenses/by-nc-nd/4.0/>), which permits use, distribution, and reproduction in any medium, provided that the Article is properly cited, the use is non-commercial, and no modifications or adaptations are made.



DETECTION OF LINE OBJECTS BY MEANS OF GABOR WAVELETS AND HOUGH TRANSFORM

U. MARMOL¹, N. BOROWIEC²

This article presents a method for detecting linear objects with a defined direction based on image and lidar data. It was decided to use Gabor waves for this purpose. The Gabor wavelet is a sinusoid modulated by the Gauss function. The orientation angle of the sinusoid means that the waveform can only operate in strictly defined directions. It should, therefore, provide an appropriate solution to the problem posed by the publication. The research problem focused in the first stage on determining the approximate location of only the analysed objects, and in the next step on correct and accurate detection. The first stage was carried out using Gabor filters, the second - using the Hough transform. The tests were performed for both laser data and image data. In both cases, good results were obtained for both stages: approximate location and precise detection.

Keywords: edge detection, line objects, Gabor wavelets, Hough transform

1. INTRODUCTION

The aim of this paper is to propose a method of edge detection with a strictly defined direction on the basis of image and laser data. Traditional filters detect edges in all directions (e.g. Canny filter) or in three selected directions - horizontal, vertical or diagonal (e.g. Roberts filter). Moreover, often only specific linear objects such as power lines, tracks or pipelines are analysed. They usually have

¹ DSc., PhD., Eng., prof. AGH, AGH University of Science and Technology, Faculty of Mining Surveying and Environmental Engineering, Al. Mickiewicza 30, 30-059 Krakow, Poland, e-mail: entice@agh.edu.pl

² DSc., PhD., Eng., AGH University of Science and Technology, Faculty of Mining Surveying and Environmental Engineering, Al. Mickiewicza 30, 30-059 Krakow, Poland, e-mail: nboro@agh.edu.pl

strictly defined directions of the course. Classical filters detect this information, of course, but also allow through a large amount of redundant data that makes further analysis difficult. The problem is shown in Fig. 1. Let us assume that in Fig. 1a) we are only looking for information about the edge marked in red. As a result of using classic filters we will obtain information about this object, but also about other objects in the surroundings. In the case of a Canny filter (Fig. 1b), we will obtain information about every edge, which makes it very difficult to analyse the selected object. Using diagonal filters (Fig. 1c), we will reduce the amount of redundant information, but it is still significant.

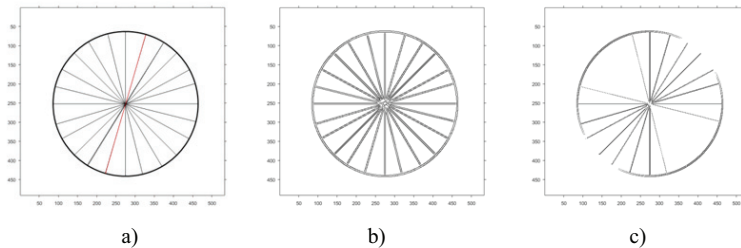


Fig. 1. Original image (a), Canny filter image (b), Roberts filter image for diagonal (c)

The problem posed by the work is to find such a solution that would allow determination of the edges only with a strictly defined direction that is responsible for the course of specific objects such as railway tracks, pipelines or power lines.

The issues of linear object detection based on photogrammetric and laser data have been discussed in many publications. The authors use complex mathematical methods based on: wavelet analysis [1], neural network algorithms [2], Radon transformations [3], Hough transform [4], RANSAC method [5],[6], height differences [7] or classification methods such as Random Forest [2] or Support Vector Machines (SVM) [8]. In their studies, the authors focus on developing an optimal algorithm for linear object detection.

The aim of this publication is not to prepare such a solution, but to propose the algorithm that would allow to reduce the research area, thus indirectly increasing the accuracy and effectiveness of other extraction methods.

It was decided to use Gabor waves for this purpose. The Gabor wavelet is a sinusoid modulated by the Gauss function. Due to this, the parameters of the Gabor function are: the frequency and orientation of the sinusoid and the scaling parameters of the Gauss function [9]. The orientation

angle of the sinusoid means that the waveform can only operate in strictly defined directions. It should, therefore, provide an appropriate solution to the problem posed by the publication.

2. THEORETICAL BASES OF GABOR WAVELETS

The Gabor wavelet was used as a filter in multichannel filtration processes. It has the features specific for these types of analyses, meaning simplicity, optimal location - both in a spatial and a frequential domain, and the ability to simulate the behaviour of receptors in the human visual system [10].

Gabor wavelets constitute an optimal basis helpful in distinguishing the features of objects for the following reasons [10]:

- biological argumentation: the shape of Gabor wavelets is similar to the receptor cells in the human visual system,
- mathematical argumentation: the Gabor transformation has both multi-resolution and multi-directional properties and it is optimal in determining the local spatial frequencies,
- empirical argumentation: Gabor wavelets were created in order to ensure the space of features that is free of deformations for tasks related to the identification of patterns.

The Gabor wavelet is a sinusoid modulated by the Gauss function. Due to this, the parameters of the Gabor function are: the frequency and orientation of the sinusoid and the scaling parameters of the Gauss function [9].

Decomposition using the family of Gabor wavelets is characterised by a local scale, orientation and phase. A single Gabor wavelet allows filtering the image while retaining only a precisely selected frequency range. The filter may be implemented both in a spatial domain by means of convolution with a calculated mask, as well as in a frequential domain.

The basic Gabor wavelet $g(x, y)$ in a spatial domain is a sinusoid with a specified frequency and orientation $s(x, y)$ (carrier), modulated by a specified window $w(x, y)$ (envelope):

$$(2.1) \quad g(x, y) = s(x, y) * w(x, y)$$

The carrier is a complex sinusoid (Fig. 2):

$$(2.2) \quad s(x, y) = \exp(i2\pi \cdot F \cdot x') = \cos((2\pi \cdot F \cdot x') + i \cdot \sin(2\pi \cdot F \cdot x')$$

where:

$F = \sqrt{u^2 + v^2}$ – the frequency of the complex sinusoid,

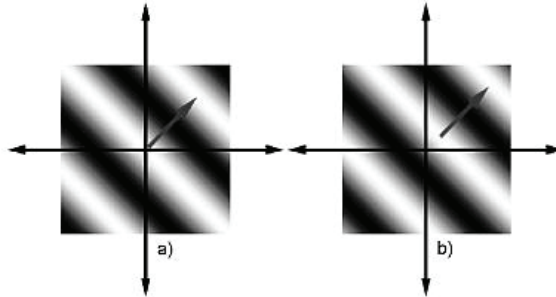


Fig. 2. The real (a) and imaginary (b) parts of the complex sinusoid. Parameters: $u = v = 1/80$ cycle/pixel

Source: [12,13]

The envelope is usually a Gauss function:

$$(2.3) \quad w(x, y) = \frac{1}{2\pi\sigma_x\sigma_y} \cdot \exp\left(-\frac{x'^2}{2\sigma_x^2} - \frac{y'^2}{2\sigma_y^2}\right)$$

where:

σ_x, σ_y – parameters scaling the axes of the Gauss function,

$$x' = (x - x_0)\cos\theta + (y - y_0)\sin\theta$$

$$y' = (x - x_0)\sin\theta + (y - y_0)\cos\theta$$

(x_0, y_0) – the centre of the Gauss function,

θ – the angle of rotation of the Gauss function around (x_0, y_0) .

Summarising, the Gabor wavelet may be written down as:

$$(2.4) \quad g(x, y) = \frac{1}{2\pi\sigma_x\sigma_y} \exp\left(-\frac{x'^2}{2\sigma_x^2} - \frac{y'^2}{2\sigma_y^2}\right) \exp(i2\pi \cdot F \cdot x')$$

2.1 GENERATING GABOR FILTERS

Objects will be properly extracted when the filter parameters are defined in the correct manner. In the case of Gabor wavelets, the following parameters should be set appropriately: frequency f , orientation angle θ and scaling parameters of the Gauss function σ_x and σ_y .

Depending on the frequency selection f object detection is performed at different levels of detail - which are defined as levels of scales s . The value θ determines the direction of the filter. The size of the Gauss function, i.e. scaling parameters σ_x, σ_y , determine the size of the window in which the analyses are performed. A set of filters differing in scale and orientation parameters is defined as a

bank of filters. Figure 3 shows an example of Gabor filter bank (real part and magnitude response) for three orientations $\theta = 0, \frac{\pi}{8}, \frac{\pi}{4}$ and three scales $s = 1, \frac{\sqrt{2}}{2}, \frac{1}{2}$.

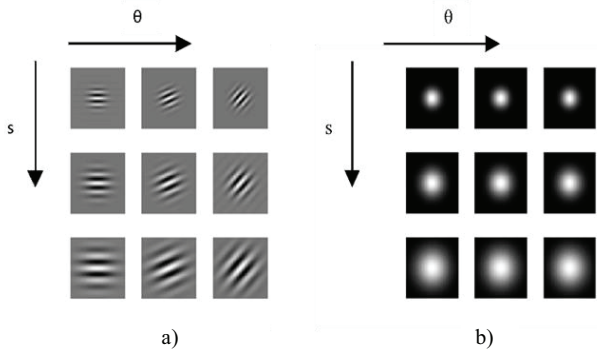


Fig. 3. Gabor filter bank - the real part (a) and the magnitude response (b). The presented example: three scales s and three orientations θ

2.2 THE EXTRACTION OF FEATURES BASED ON THE RESPONSE OF GABOR FILTERS

During the next stage, the filter images undergo an analysis intended to extract the selected features describing the individual objects. Numerous methods were developed for this action. Among the most crucial, one may list algorithms that use:

- filter response (magnitude response) [14],
- the real component of the filter Re [15],
- a sigmoid function [15].

In this paper, it has been decided to select the filter response. The filter response is expressed by the formula:

$$(2.5) \quad M_f = abs(G_f)$$

where $G(f)$ is a Gabor transformation of the analysed image $f(x,y)$. This is created by convolution of the image by applying Gabor wave $g(x,y)$ functions (Eq.2.4) [16].

3. THEORETICAL BASICS OF THE HOUGH TRANSFORMATION FOR A STRAIGHT LINE

The idea of the classical Hough transform (HT) is based on the observation of symmetry of the equation of directional straight line defined by the formula [17]:

$$(3.1) \quad y_i = ax_i + b$$

where:

a - is the directional coefficient equal to the tangent of the angle between the line and the axis Ox,

b - a free word equal to the ordinate of the point at which the line intersects the axis Oy.

This equation, in the Cartesian space, is fulfilled by each pair of points (x_i, y_i) lying on a single line. Thus, one pair of parameters (a, b) is enough to define a straight line in the coordinate space. Therefore, its representation in the space of parameters is a point (Fig. 4a). To obtain a formula for mapping a given point (x, y) to Hough's space, it is enough to change the meaning of parameters and variables of the above equation to the form: $b_i = -xa_i + y$.

The transformed formula also has the form of the directional straight equation, which means that a point with fixed coordinates (x, y) in the Cartesian space is mapped in the space of parameters as a straight line (Fig. 4b). Finding a solution to the above equation, i.e. the set of points (a_i, b_i) , corresponds to determining the parameters of all possible straight lines (a bunch of straight lines) passing through the mapped point (x, y) .

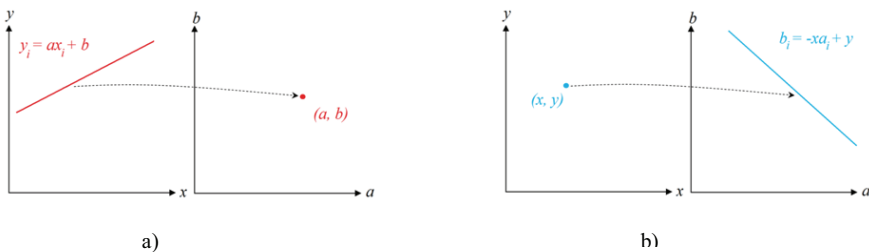


Fig. 4. (a) Straight line in coordinate space and parameter space, (b) Point in coordinate space and parameter space

On the basis of the above theses, it can be concluded that collinear points in the space of coordinates are represented in the space of parameters as lines, intersecting in one point (Fig. 5).

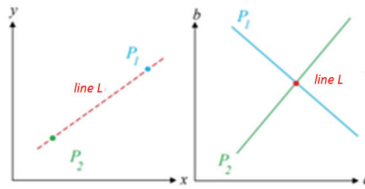


Fig. 5. Collinear points in coordinate space and parameter space

3.1. HOUGH TRANSFORM USING THE NORMAL STRAIGHT EQUATION

The use of the straight directional equation for parameterization has one major disadvantage: parameters a and b have an infinite range of values, because the direction of the line can change from horizontal to vertical. Richard Duda and Peter Hart in their work [18] proposed an alternative way of parametrising straight lines using the normal equation:

$$(3.2) \quad x_i \cdot \cos\theta + y_i \cdot \sin\theta = \rho \Leftrightarrow y_i = -\frac{\cos\theta}{\sin\theta} \cdot x_i + \frac{\rho}{\sin\theta}$$

where:

θ – the angle between the positive axis of the ordinates and the normal axis of the line,

ρ – radius, equal to the line distance from the beginning of the coordinate system.

As in the case of the directional equation, one pair of parameters (θ, ρ) is enough to determine the line in the Cartesian space – therefore, its image in the parametric space is a point (Fig. 6a). However, a point with fixed coordinates in the Cartesian space is represented in Hough's space as a sinusoidal curve, according to the normal equation of a straight line (Fig. 6b).

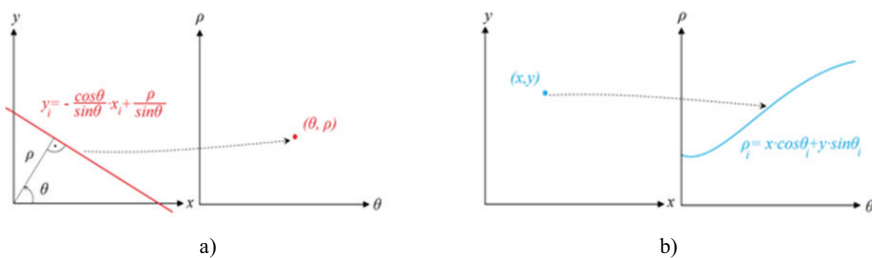


Fig. 6. a) A straight line in coordinate space (x,y) and parameter space (θ, ρ) . (b) Point in coordinate space (x,y) and in parameter space (θ, ρ)

Collinear points in the Cartesian system are represented in space (θ, ρ) as sinuses, intersecting at one point (Fig. 7).

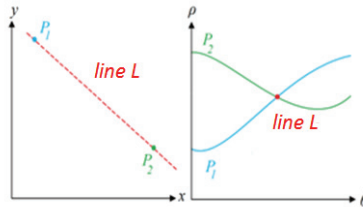


Fig. 7. Collinear points in coordinate space (x,y) and parameter space (θ, ρ)

If the range θ is narrowed down to $[0, \pi]$, then the parameters (θ, ρ) of the line become unique [18]. According to this assumption, each line in the Cartesian space corresponds to one point in the parameter space. Thanks to the defined, finite ranges of parameters, it was possible to implement and calculate the Hough transformation in computer systems.

3.2. ACCUMULATOR TABLE

Hough's transformation is implemented through the division of continuous space (ρ, θ) for the collection of finite cells, called accumulators. Initially, all the cells in the array are reset to zero. Then, during the operation of the algorithm, each image point is transformed into a discrete sinusoidal curve in space (ρ, θ) . Calculated values ρ for a sequence of parameter values $\theta \in (0, 2\pi)$ are marked by entering parameter values in appropriate places in the array (adding one value when a cell has a number, entering one when a cell is empty). As a result, if many sine waves pass through a cell, it will reach a relatively high value in comparison with neighbouring cells. Consequently, the local maximum in space (ρ, θ) corresponds to each line in the image. Moreover, the position of the cell is determined by the parameters of the corresponding line, and its height by the length of the line.

3.3. HT AND STRAIGHT LINE DETECTION IN IMAGES

When analysing images, the x and y coordinates of a point (pixel) in equation (3.1) are constant, while ρ and θ are variables wherein for each successive angle value θ , the corresponding value ρ is determined from the formula (3.1). As a result, each point (x,y) - a pixel - has a sinusoidal curve in

space (ρ, θ) . If there are two or more collinear pixels in the image, the corresponding sine waves intersect at one point. The coordinates (ρ, θ) of this point are given by the parameters of the line along which the collinear pixels are situated.

A slightly improved Hough's transformation was used in the study [19]. This transformation, compared to the standard Hough transformation, allows determining and obtaining higher angular and radial resolution of the found lines. At the same time, it is also possible to ascertain the number of local maxima that actually determines the number of lines to be detected.

4 THE CONCEPT OF LINE DETECTION ON THE RASTER IMAGE

Based on the analysis of the literature and our own research, the authors developed an algorithm that is precisely detect artificial construction line elements on an orthophotomap and pseudorasters obtained from airborne laser data. This method consists of several steps. In the first step, it is possible to build an image that determines the direction and place of the line elements by using Gabor filters. The resulting image is used to build a mask, which is minimize the field of precise indication of the line. Before building the mask, noise is removed, i.e. small clusters of pixels. Removing all the small "black boxes" is possible by counting the number of pixels of each figure, and the figures with the smallest field are removed. The next step is segmentation (binarization) of the image, i.e. division into two areas - the object (mask) and the background. The object is the entire area bounded by lines detected with a Gabor filter. Finding this area is possible by applying image after removing the noise to the input image (orthophotomap or pseudoraster from lidar data). Then the values of superimposed pixels are added, if the sum has not increased, the pixel in the resulting image is assigned the value zero, the remaining pixels value one. To fill the figure (obtain the mask), morphological filters are used in the close - open combination. By applying a mask to the input image, only areas containing linear objects can be acquired. In the next step, the image is binarized again by means of a threshold. The thresholds are determined individually for each input image based on the histogram. If the images are still noisy, then a minimum filter is used to improve quality. In the image that obtained, the precise indication of the course line is possible by the Hough transform. The image processing scheme is shown below in Fig.8

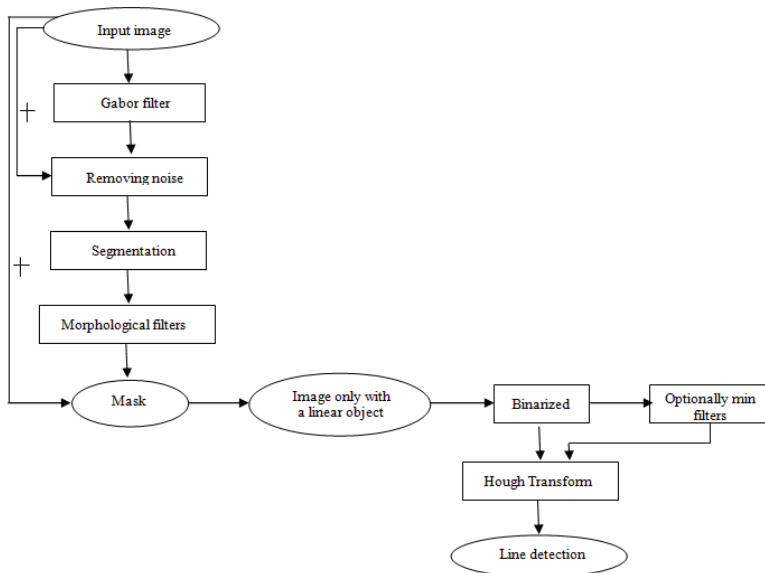


Fig. 8. Image processing flowchart

The developed concept was applied to three test fields. The test fields are areas that covered linear elements of the construction infrastructure, i.e. power lines, pipelines and railway tracks.

5 TEST FIELD 1: POWER LINES

In the initial stage of the research, the focus was on power lines registered with the ALS system. The first test field was selected as an area of the size: 250 x 85 m. Using the information on average density of points, two grids with a 0.1 m cell - DTM and DSM - were interpolated. The method of the nearest neighbour was used. This does not introduce smoothing of data, because in this case it would disturb the information about power lines. By subtracting the above models, the nDSM was obtained. Visualisation of the area is shown in Fig. 9.

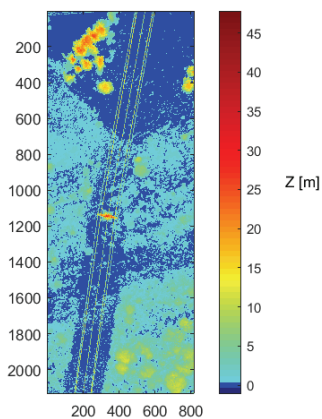


Fig. 9. Test field 1 - nDSM

5.1. DETERMINATION OF APPROXIMATE POSITION OF POWER LINES

The task set is to extract only the course of power lines from the analysed area. The use of traditional edge filters allows the extraction of lines, but together with these, all the edge objects in the test field are extracted as well. The result of using traditional Canny and Roberts filters is shown in Figure 10. As can be seen, the image of the power line is made noisy by the edges of the surrounding trees.

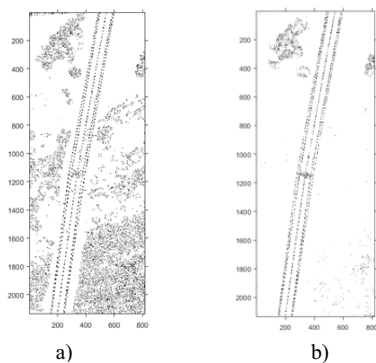


Fig. 10. Edges detected by Canny (a) and Roberts (b) filter (for 45° angle)

The following steps were carried out using the theory presented in Chapter 2. A Gabor filter was designed so as to determine the following parameters: $f = \frac{1}{4}$, $\theta = 80^\circ$, while the Gauss function scaling parameters $\sigma_x, \sigma_y = 8$ pixels.

The obtained result was thresholded and the final result of power line extraction is shown in Fig. 11.

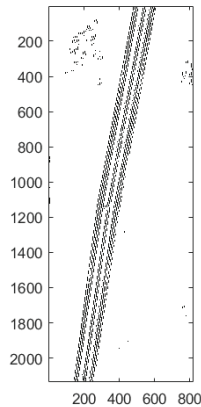


Fig. 11. Result of power line extraction after applying a Gabor filter

As can be seen from Figure 11, the applied methodology allowed determining the approximate course of the power line, and it significantly reduced information about other objects.

5.2. PRECISE DETECTION OF THE POWER LINE

Prior to the precise determination of the Hough's transformation course of power lines, the group of pixels in the upper side was removed and the area representing the line sequence was cut out of the original image. The cut-out was made using a defined mask. The mask (Fig. 12) is presented in where the two sides are the lines obtained using the Gabor filter. As a result of applying the mask to the input raster (DSM), an image is obtained where only the power lines are visible. Then the raster was binarized (Fig. 13). When defining HT parameters, 5 local maxima were determined at the beginning, which means that a maximum of 5 elements representing collinear pixels should be detected. The lines were detected but did not reflect the actual course of the power lines. Therefore, it was decided to increase the number of local maxima to 15. The detected lines are shown in Figure 14 in full and in enlargements in Figure 14 a, b.

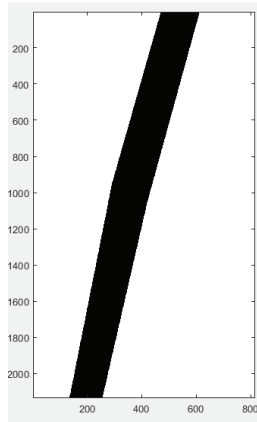


Fig. 12. Mask image for power lines

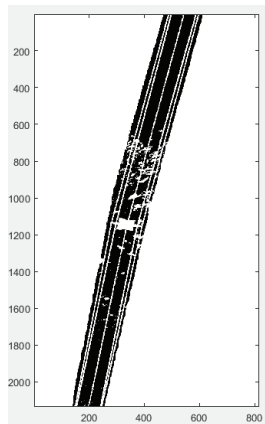


Fig. 13. Binary image only with power lines

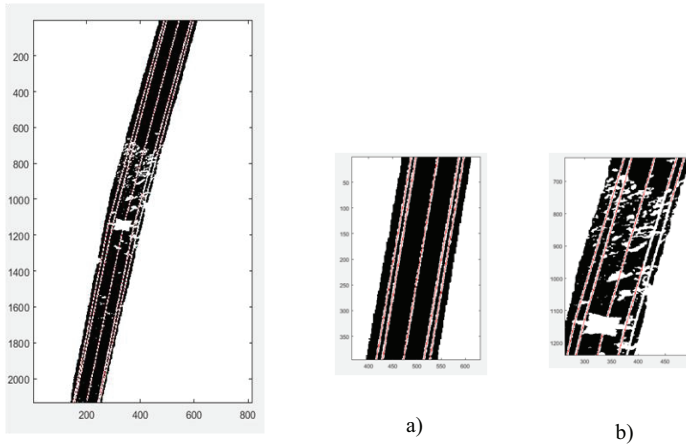


Fig. 14. Binary image with detected using HT power lines (red lines). (a),(b) - enforcements selected areas
The image shows that all lines were correctly detected on almost their entire length thanks to the Hough transform. Errors appear at the traction pole, there the lines were interrupted, because the high vegetation overshadowed the pole at this point.

6 TEST FIELD 2: RAILWAY TRACKS

A fragment of railway tracks passing through an urban area was selected as another example. This time, image data was used, i.e. an orthophotomap with a terrain pixel equal to 10 cm. The research area is shown in Figure 15.



Fig. 15. Orthophotomap with test field 2

6.1. DETERMINATION OF APPROXIMATE POSITION OF RAILWAY TRACKS

In the first step, edge extraction was carried out using classic Canny and Roberts filters. The obtained results are presented in Fig. 16.

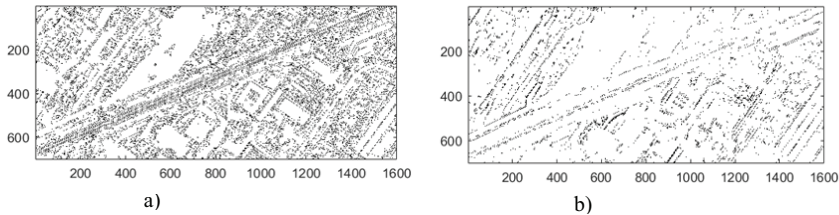


Fig. 16. Canny (a) and Roberts (b) filter results

The analysis of the railway infrastructure in these cases is very difficult due to the presence of all the other edges located in the area. Even the extraction of the edges with a diagonal filter (Roberts filter) the information about the tracks still poorly readable.

A Gabor filter was then applied using the following parameters: $f = \frac{1}{2}$, $\theta = 20^\circ$ i $\sigma_x, \sigma_y = 8$ pixels.

The results are shown in 17.

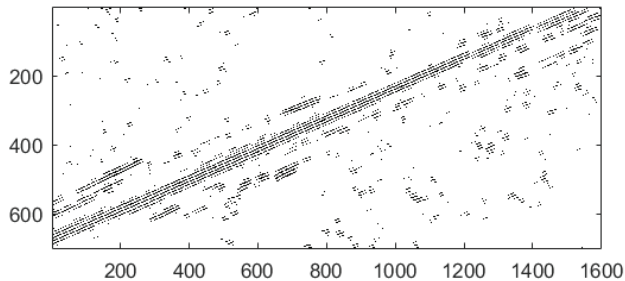


Fig. 17. The result of using a Gabor filter for test field 2

6.2. PRECISE DETECTION OF RAILWAY TRACKS

The use of a Hough's transformer in developing the mapping of the railway tracks is more complex than in the previous case. After applying Gabor's filter, the image is very noisy. Therefore, it was

decided to first remove clusters larger than 100 pixels in order to best determine the course of the railway tracks. Based on the resulting image, a mask was built (Fig. 18). The mask was used to cut the location of the track from the orthophotomap (Fig. 19). This treatment limits the place of detection and correct determination of railway tracks. Then image thresholding was performed to obtain a binary image (Fig. 20).

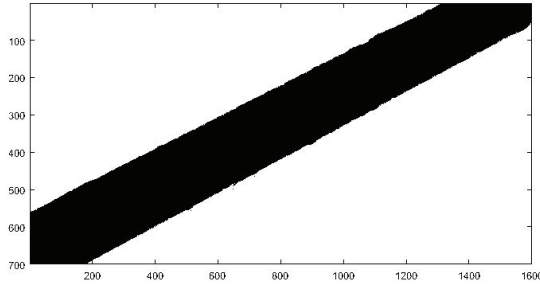


Fig. 18. Mask image for railway tracks

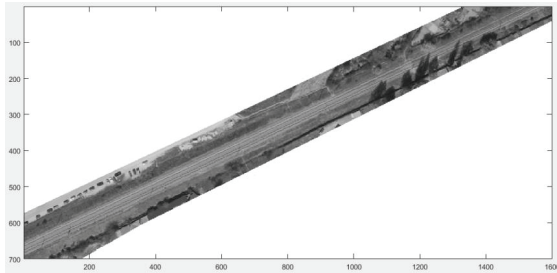


Fig. 19. Fragment of the orthophotomap representing railway traction, cut out when applying the mask

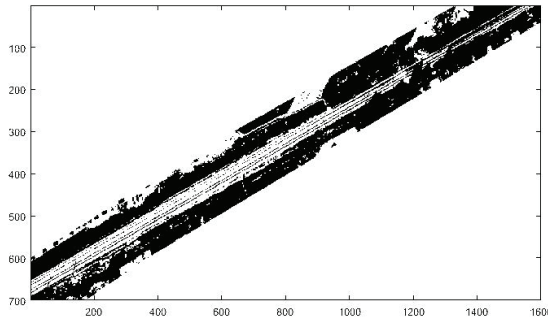


Fig. 20. Binary image of railway tracks

In the next step, the number of local maxima was defined to determine the number of railway tracks. Only fragments of the railway track from the west towards the center were correctly detected in the image, whose course is determined by a continuous line. In places where there was a break in the linearity of pixels, i.e. in places where the tracks were obstructed by tall trees, also the straight defined HT did not maintain continuity and was detected (Fig. 21).

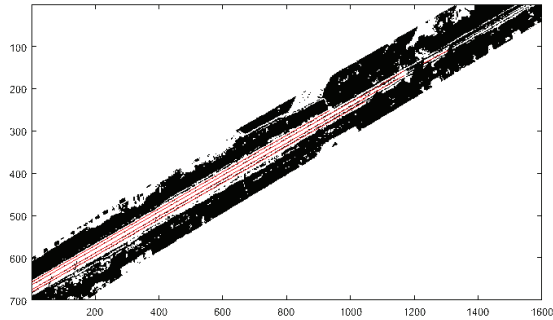


Fig. 21. Binary image with detected lines using Hough transform (red lines)

7 TEST FIELD 3: PIPELINE

In the next stage of the research, an area with a more complex course of linear objects was selected. Herein, a pipeline was identified which had changes in the run of its trajectory in the analysed area. The research was conducted on an orthophotomap with a terrain pixel equal to 0.25 m. The test field is shown in Figure 22.



Fig. 22. The test field 3 containing the fragment of the pipeline

7.1. DETERMINATION OF APPROXIMATE POSITION OF THE PIPELINE

Similarly to the previous examples, traditional Canny and Roberts filters were applied and the results assessed. Figure 23 shows the results obtained, which prove once again that the use of classic filters generates a lot of redundant information.

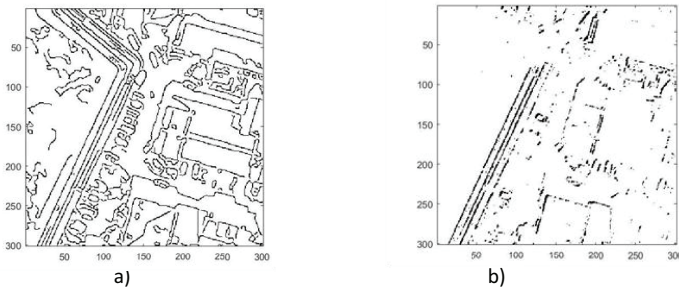


Fig. 23. Edges detected by Canny (a) and Roberts (b) filters

Due to the fact that in the above case, the pipeline has changes in direction within the analyzed area, it was necessary to generate not a single filter, but a Gabor filter bank with specific parameters. The filters contained in the bank differed in parameter θ . Simultaneous filtration was performed for the test field using a bank built of two filters for $\theta=65^\circ$ i $\theta=140^\circ$. Other parameters were adopted as $f = \frac{1}{4}$ i $\sigma_x, \sigma_y = 8$ pixels. The result is shown in Figure 24.

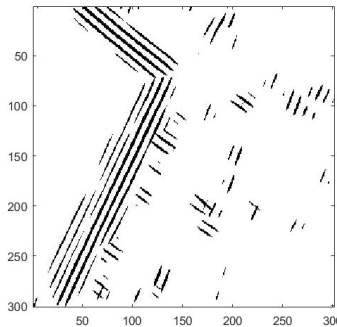


Fig. 24. Edges detected by means of a generated Gabor filter bank

7.2. PRECISE DETECTION OF THE PIPELINE

In order to correctly detect the course of the pipeline, as in previous cases, a mask was built on the basis of the image with the detected edges of the applied Gabor's filter. The resulting mask was composed of two masks, which respectively defined the course of the pipelines (Fig. 25). Then, using the composite mask, only the area presenting the pipelines was cut out of the input image. In the grayscale image (Fig. 26), a threshold was selected in order to obtain a binary image (Fig. 27). The detected pipeline presentation areas were, however, too wide, so it was decided to use a minimum filter on the image that reduced the width of the pipelines (Fig. 28). The next step was to determine the number of maxima, i.e. the number of lines to be detected. The value was rounded to 4, because there are so many main pipe runs. Unfortunately, not all the lines representing collinear pixels were detected. It was decided to increase this number to 6. This procedure gave satisfactory results by detecting pipeline centers, although it detected pipeline centers because a minimum filter was used, which reduced the area but also prevented detection double strings of pipes (Fig. 29). The algorithm managed to cope despite the change of direction of the pipelines, however, the lines are broken.

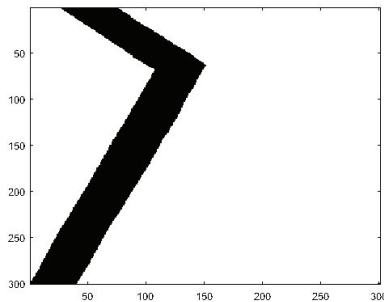


Fig. 25. Mask image for the pipeline

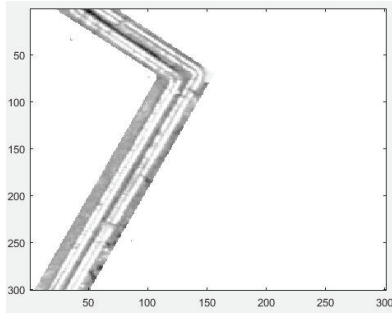


Fig. 26. Part of the orthophotomap representing the pipeline cut out when applying the mask

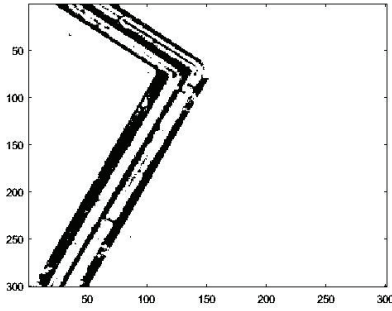


Fig. 27. Binary image of the pipeline

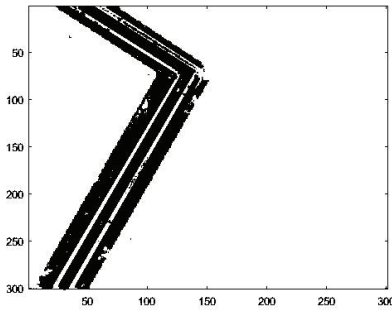


Fig. 28. Binary image where use minimum filter

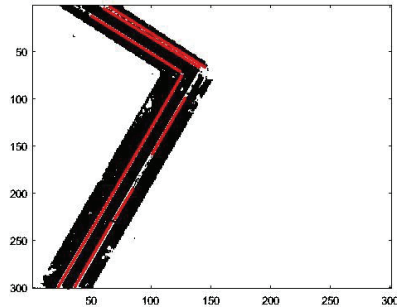


Fig. 29. Binary image with detected lines using Hough transform

8. SUMMARY AND CONCLUSIONS

The purpose of the article was to assess the automatic extraction of linear objects using laser and image data. The research problem focused in the first stage on determining the approximate location of only the analysed objects, and in the next step on correct and accurate detection. The first stage was carried out using Gabor filters, the second - using the Hough transform. The tests were performed for both laser data and an orthophotomap. In both cases, good results were obtained for stages: approximate location and precise detection.

Gabor wavelets due to the specifics of their construction can operate in strictly defined directions - this is controlled using a parameter θ . The second important advantage of wavelets is the ability to generate a filter bank, i.e. a set of filters, differing in specific parameters. In this approach, the analysed area is modified not with a single filter, but with a set of filters that operate in differently. Subsequently, a filter bank can be constructed to extract only the desired information from the input data. The conducted research revealed the great potential of the methodology for use in the detection of linear objects. The approximate location of the objects has been correctly determined for all test fields.

In the precise location of the line elements using HT, it is important to extract only the places representing the line elements from the images. Therefore, the use of masks based on Gabor's filter significantly reduce the field of line searches. The biggest problems occurred in the second case, where, in the image, after applying the mask and performing threshold, the lines were not continuous. For each sequence of collinear pixels, a separate straight line was determined using Hough's transformation. In the third case, despite the change of line direction, the algorithm did well.

The work started in this article will be continued in order to fully automate the data processing. Further stages of the research will focus on an attempt to automatically select Gabor filter parameters and Hough transform parameters.

ACKNOWLEDGEMENT: The article was prepared under the research subvention of AGH University of Science and Technology No. 16.16.150.545.

REFERENCES

- [1] A. Fryskowska, Improvement of 3D Power Line Extraction from Multiple Low-Cost UAV Imagery Using Wavelet Analysis, *Sensors (Basel)* 19(3):700, 2019.
- [2] Y. Wang, Q. Chen, L. Liu, X. Li, A. K. Sangaiah, K. Li, Systematic Comparison of Power Line Classification Methods from ALS and MLS Point Cloud Data, *Remote Sensing* 10(8): 1222, 2018.
- [3] G. Yan, C. Li, G. Zhou, W. Zhang, X. Li, Automatic Extraction of Power Lines From Aerial Images, *IEEE Geoscience and Remote Sensing Letters*, 4(3): 387-391, 2007.
- [4] M. Yermo, J. Martínez, O. G. Lorenzo, D. L. Vilarinho, J. C. Cabaleiro, T. F. Pena, F. F. Rivera, Automatic detection and characterisation of power lines and their surroundings using lidar data, *International Archives of the Photogrammetry, Remote Sensing and Spatial Information Sciences*, XLII-2/W13:1161–1168, 2019.
- [5] R. Zhou, W. Jiang, S. Jiang, A Novel Method for High-Voltage Bundle Conductor Reconstruction from Airborne LiDAR Data, *Remote Sensing* 10(12):2051, 2018.
- [6] B. Guo, Q. Li, X. Huang, C. Wang, An improved method for power-line reconstruction from point cloud data, *Remote Sensing* 8(1):36, 2016.
- [7] M. Awrangjeb, Extraction of Power Line Pylons and Wires Using Airborne LiDAR Data at Different Height Levels. *Remote Sensing* 11(15):1798, 2019.
- [8] Y. Wang, Q. Chen, L. Liu, D. Zheng, C. Li, and K. Li, Supervised classification of power lines from airborne lidar data in urban areas, *Remote Sensing* 9(8): 771, 2017.
- [9] J. N. Niya, A. Aghagolzadeh, M. A. Tinat, S. Feizi, 2-step wavelet-based edge detection using gabor and cauchy directional wavelets, *The 7th International Conference on Advanced Communication Technology, ICACT 2005*.
- [10] J. G. Daugman, Uncertainty relation for resolution in space, spatial-frequency, and orientation optimized by two-dimensional visual cortical filters, *J. Opt. Soc. Amer.* 2: 1160-1169, 1985.
- [11] L. Shen, L. Bai, A review of Gabor wavelets for face recognition, *Pattern Analysis and Applications* 9: 273-292, 2006.
- [12] J. Movellan, Tutorial on Gabor Filters, Open source document. 2002.
- [13] M. Włodarczyk, T. Matuszczak, Rozpoznawanie człowieka przy pomocy wzorca tęczówki oka, Raport z projektu kursu metody i algorytmy sztucznej inteligencji, Politechnika Wrocławska, 2009.
- [14] A. C. Bovik, M. Clark, W. S. Geisler, Multichannel texture analysis using localized spatial filters, *IEEE Trans. Pattern Analysis Mach. Intell.* 12: 55-73, 1990.
- [15] A. K. Jain, F. Farrokhnia, Unsupervised texture segmentation using gabor filters, *Pattern Recognition* 16: 1167-1186, 1991.
- [16] F. Bergeaud, S. Mallat, Matching pursuit of images, *Proc. SPIE* 2491, *Wavelet Applications II*: 1-16, 1995.
- [17] M. Nixon, A. Aguado, *Feature extraction and Image processing*, Second Edition. Elsevier Ltd., Oxford, 2008.
- [18] R. Duda, P. Hart. Use of the Hough Transformation to detect lines and curves in pictures, *Communications ACM* 15: 11-15, 1972.
- [19] A. Anagnou, J. M. Blackledge, *Pattern Recognition using the Hough Transform*, Sciences and Engineering Research Centre, De Montfort University, Leicester 1993.

LIST OF FIGURES AND TABLES:

Fig. 1. Original image (a), Canny filter image (b), Roberts filter image for diagonal (c)

Rys. 1. Obraz oryginalny (a), filtr Canny'ego (b), filtr Robertsa (c)

Fig. 2. The real (a) and imaginary (b) parts of the complex sinusoid. Parameters: $u = v = 1/80$ cycle/pixel

Rys. 2. Część rzeczywista (a) i urojona (b) zespolonej sinusoidy. Parametry: $u = v = 1/80$ cykli/piksel

Fig. 3. Gabor filter bank - the real part (a) and the magnitude response (b). The presented example: three scales s and three orientations θ

Rys. 3. Bank filtrów Gabora – część rzeczywista (a) i odpowiedź filtru (b). Prezentowany przykład: trzy skale s i trzy orientacje θ

Fig. 4. a) Straight line in coordinate space and parameter space, b) Point in coordinate space and parameter space

Rys. 4. a) Linia prosta w przestrzeni współrzędnych oraz w przestrzeni parametrów b) Punkt w przestrzeni współrzędnych oraz w przestrzeni parametrów

Fig. 5. Collinear points in coordinate space and parameter space

Rys. 5. Punkty kolinearne w przestrzeni współrzędnych i przestrzeni parametrów

Fig. 6. a) A straight line in coordinate space (x,y) and parameter space (θ, ρ) . (b) Point in coordinate space (x,y) and in parameter space (θ, ρ)

Rys. 6. a) Linia prosta w przestrzeni współrzędnych (x,y) oraz w przestrzeni parametrów (θ, ρ) . (b) Punkt w przestrzeni współrzędnych (x,y) oraz w przestrzeni parametrów (θ, ρ) .

Fig. 7. Collinear points in coordinate space (x,y) and parameter space (θ, ρ)

Rys. 7. Punkty współliniowe w przestrzeni współrzędnych (x,y) i przestrzeni parametrów (θ, ρ)

Fig. 8. Image processing flowchart

Rys. 8. Schemat przetworzeń obrazów

Fig. 9. Test field 1 - nDSM

Rys. 9. Pole testowe 1 - ZNMPT

Fig. 10. Edges detected by Canny (a) and Roberts (b) filter (for 45° angle)

Rys. 10. Krawędzie wykryte filtrem Canny'ego (a) i Roberts'a (b) (dla kąta 45°)

Fig. 11. Result of power line extraction after applying a Gabor filter

Rys. 11. Wynik ekstrakcji linii energetycznej z wykorzystaniem filtru Gabora

Fig. 12. Mask image for power lines

Rys. 12. Maska dla linii energetycznych

Fig. 13. Binary image only with power lines

Rys. 13. Obraz binarny wyłącznie z liniami energetycznymi

Fig. 14. Binary image with detected using HT power lines (reds lines). a, b - enlargements selected areas

Rys. 14. Obraz binarny z wykrytymi za pomocą HT liniami energetycznymi (czerwone linie). a, b - powiększone wybrane obszary

Fig. 15. Orthophotomap with test field 2

Rys. 15. Ortofotomapa z polem testowym 2

Fig. 16. Canny (a) and Roberts (b) filter results

Rys. 16. Wyniki filtru Canny'ego (a) i Roberts'a (b)

Fig. 17. The result of using a Gabor filter for test field 2

Rys. 17. Wynik wykorzystania filtru Gabora dla pola testowego 2

Fig. 18. Mask image for railway tracks

Rys. 18. Maska dla torów kolejowych

Fig. 19. Fragment of the orthophotomap representing railway traction, cut out when applying the mask

Rys. 19. Fragment ortofotomapy przedstawiający trakcję kolejową, wycięty poprzez zastosowanie maski

Fig. 20. Binary image of railway tracks

Rys. 20. Obraz binarny torów kolejowych

Fig. 21. Binary image with detected lines using Hough transform (red lines)

Rys. 21. Obraz binarny z wykrytymi liniami z wykorzystaniem transformaty Hougha (czerwone linie)

Fig. 22. The test field 3 containing the fragment of pipeline

Rys. 22. Pole testowe 3 zawierające fragment rurociągu

Fig. 23. Edges detected by Canny (a) and Roberts (b) filters

Rys. 23. Krawędzie wykryte przez filtry Canny'ego (a) i Roberts'a (b)

Fig. 24. Edges detected by means of a generated Gabor filter bank

Rys. 24. Krawędzie wykryte za pomocą wygenerowanego banku filtrów Gabora

Fig. 25. Mask image for the pipeline

Rys. 25. Maska dla rurociągu

Fig. 26. Fragment of the orthophotomap representing the pipeline cut out when applying the mask

Rys. 26. Fragment ortofotomapy przedstawiający rurociąg wycięty poprzez zastosowanie maski

Fig. 27. Binary image of the pipeline

Rys. 27. Obraz binarny rurociągu

Fig. 28. Binary image where use minimum filter

Rys. 28. Obraz binarny, w którym zastosowano filtr minimalny

Fig. 29. Binary image with detected lines using Hough transform

Rys. 29. Obraz binarny z wykrytymi liniami z wykorzystaniem transformaty Hougha

DETEKCJA OBIEKTÓW LINIOWYCH Z WYKORZYSTANIEM FALEK GABORA I TRANSFORMATY HOUGHA

Słowa kluczowe: detekcja krawędzi, obiekty liniowe, falki Gabora, transformata Hougha

STRESZCZENIE:

Celem pracy jest zaproponowanie metody wykrywania krawędzi o ściśle określonym kierunku przebiegu na danych obrazowych i laserowych. Tradycyjne filtry wykrywają krawędzie we wszystkich kierunkach (np. filtr Canny), ewentualnie w trzech wybranych – horyzontalnym, wertykalnym lub diagonalnym (np. filtr Roberts).

Często przedmiotem analiz są tylko określone obiekty liniowe jak linie energetyczne, tory, czy rurociągi. Mają one zazwyczaj ściśle określone kierunki przebiegu. Klasyczne filtry wykrywają oczywiście te informacje, ale także dużą ilość danych nadmiarowych, które utrudniają dalsze analizy.

Problemem postawionym w pracy jest znalezienie takiego rozwiązania, które pozwoliłoby na wyznaczenie krawędzi tylko i wyłącznie o ściśle określonym kierunku, odpowiadających za przebieg konkretnych obiektów takich jak tory kolejowe, rurociągi czy linie energetyczne.

Problem badawczy skupiał się w pierwszym etapie na określeniu przybliżonej lokalizacji wyłącznie analizowanych obiektów, a w kolejnym kroku na poprawnej i dokładnej ich detekcji. Pierwszy etap został przeprowadzony z wykorzystaniem filtrów Gabora, drugi - z użyciem transformaty Hougha. Testy zostały wykonane zarówno dla danych laserowych jak i danych obrazowych w postaci ortofotomapy. W obydwu przypadkach uzyskano dobre rezultaty dla obydwóch etapów: przybliżonej lokalizacji i precyzyjnej detekcji.

Falki Gabora ze względu na specyfikę ich budowy mogą działać w ściśle określonych kierunkach - jest to kontrolowane za pomocą parametru θ . Drugą ważną zaletą falek jest możliwość generowania banku filtrów, tj. zestawu filtrów, różniących się określonymi parametrami. W takim podejściu analizowany obszar nie jest modyfikowany za pomocą pojedynczego filtra, ale za pomocą zestawu filtrów, z których każdy działa w inny sposób. Bank filtrów może być zbudowany w celu wydobywania tylko pożądaných informacji z danych wejściowych. Przeprowadzone badania ujawniły duży potencjał metodologii stosowanej w wykrywaniu obiektów liniowych. Przybliżone położenie obiektów zostało poprawnie określone dla wszystkich pól testowych.

W dokładnej lokalizacji elementów liniowych za pomocą HT ważne jest, aby wyodrębnić tylko obrazy reprezentujące elementy liniowe z obrazów. Dlatego użycie masek opartych na filtrze Gabora znacznie zmniejszyło pole wyszukiwania linii. Największe problemy wystąpiły w drugim przypadku, w którym na zdjęciu po zastosowaniu maski i wykonaniu progu linie nie były ciągłe. Dla każdej sekwencji pikseli współliniowych wyznaczono osobną linię prostą za pomocą transformacji Hougha. W trzecim przypadku, pomimo zmiany kierunku linii, algorytm działał dobrze.

Prace rozpoczęte w tym artykule będą kontynuowane w celu pełnej automatyzacji przetwarzania danych. Dalsze etapy badań skupią się na próbie automatycznego wyboru parametrów filtra Gabora i parametrów transformaty Hougha.

Received: 17.02.2020 Revised: 21.05.2020

